Ramakrishna Mission Residential College (Autonomous)
Kolkata 700103, WB, India

Collaborative research in coordination chemistry of organic radicals

Number 6

Institute 1: Ramakrishna Mission Residential College (Autonomous)

Concerned Faculty: Dr. Prasanta Ghosh, Dept of Chemistry

&

Institute 2: **Max-Planck-Institut für Chemische Energiekonversion**

Stiftstrasse 34 - 36 / D - 45470 Mülheim an der Ruhr

Concerned Scientist: Dr Thomas Weyhermüller

Period of Investigation: 01-11-2015 to 27-04-2016

Project: Radical states of the [OS(PIQ)] core in complexes (PIQ = 9,10-phenanthreneiminoquinone)

Output: The result was published in the journal of international repute

Publication: Radical and Non-Radical States of the [Os(PIQ)] Core (PIQ = 9,10-Phenanthreneiminoquinone): Iminosemiquinone to Iminoquinone Conversion Promoted o-Metalation Reaction

Sachinath Bera, Sandip Mondal, Suvendu Maity, Thomas Weyhermüller and Prasanta Ghosh*

Inorg. Chem., 2016, *55*, 4746-4756.

Dr. Prasanta Ghosh

Dr Thomas Weyhermüller

Inorganic Chemistry

Article

pubs.acs.org/IC

Radical and Non-Radical States of the [Os(PIQ)] Core (PIQ = 9,10-Phenanthreneiminoquinone): Iminosemiquinone to Iminoquinone Conversion Promoted *o*-Metalation Reaction

Sachinath Bera,[†] Sandip Mondal,[†] Suvendu Maity,[†] Thomas Weyhermüller,[‡] and Prasanta Ghosh*[,†]

[†]Department of Chemistry, R. K. Mission Residential College, Narendrapur, Kolkata 103, India

[‡]Max-Planck-Institut für Chemische Energiekonversion, Stiftstrasse 34-36, D-45470 Mülheim, Germany

Supporting Information

ABSTRACT: The coordination and redox chemistry of 9,10-phenanthreneiminoquinone (PIQ) with osmium ion authenticating the $[Os^{II}(PIQ^{\bullet-})]$, $[Os^{III}(PIQ^{\bullet-})]$, $[Os^{III}(C,N\text{-}PIQ)]$, $[Os^{III}(PIQ)]$, and $[Os^{III}(PIQ^{2-})]$ states of the [Os(PIQ)] core in the complexes of types *trans*-$[Os^{II}(PIQ^{\bullet-})(PPh_3)_2(CO)Br]$ (**1**), *trans*-$[Os^{III}(PIQ^{\bullet-})(PPh_3)_2Br_2]$ (**2**), *trans*-$[Os^{III}(C,N\text{-}PIQ)(PPh_3)_2Br_2]\cdot 2CH_2Cl_2$ ($3\cdot 2CH_2Cl_2$), *trans*-$[Os^{III}(C,N\text{-}PIQ^{Br})(PPh_3)_2Br_2]\cdot 2CH_2Cl_2$ ($4\cdot 2CH_2Cl_2$), *trans*-$[Os^{III}(C,N\text{-}PIQ^{Cl2})(PPh_3)_2Br_2]$ (**6**), *trans*-$[Os^{III}(PIQ^{\bullet-})(PPh_3)_2Br_2]^+1/2I_3^-1/2Br^-$ ($1^+1/2I_3^-1/2Br^-$), $[Os^{III}(PIQ)(PPh_3)_2Br_2]^+$ (2^+), and $[Os^{III}(PIQ^{2-})(PPh_3)_2Br_2]^-$ (2^-) are reported ($PIQ^{\bullet-}$ = 9,10-phenanthreneiminosemiquinonate anion radical; C,N-PIQ = ortho-metalated PIQ, C,N-PIQ^{Br} = ortho-metalated 4-bromo PIQ, and C,N-PIQ^{Cl2} = ortho-metalated 3,4-dichloro PIQ). Reduction of PIQ by $[Os^{II}(PPh_3)_3(H)(CO)Br]$ affords **1**, while the reaction of PIQ with $[Os^{II}(PPh_3)_3Br_2]$ furnishes **2**. Oxidation of **1** with I_2 affords $1^+1/2I_3^-1/2Br^-$, while the similar reactions of **2** with X_2 (X = I, Br, Cl) produce the ortho-metalated derivatives $3\cdot 2CH_2Cl_2$, $4\cdot 2CH_2Cl_2$, and **6**. PIQ and PIQ^{2-} complexes of osmium(III), 2^+ and 2^-, are generated by constant-potential electrolysis. However, 2^+ ion is unstable in solution and slowly converts to **3** and partially hydrolyzes to *trans*-$[Os^{III}(PQ^{\bullet-})(PPh_3)_2Br_2]$ (2_{PQ}), a $PQ^{\bullet-}$ analogue of **2**. Conversion of $2^+ \rightarrow 3$ in solution excludes the formation of aryl halide as an intermediate for this unique ortho-metalation reaction at 295 K, where PIQ acts as a redox-noninnocent ambidentate ligand. In the complexes, the $PIQ^{\bullet-}$ state where the atomic spin is more localized on the nitrogen atom is stable and is more abundant. The reaction of 2_{PQ} with I_2 does not promote any ortho-metalation reaction and yields a PQ complex of type *trans*-$[Os^{III}(PQ)(PPh_3)_2Br_2]^+I_5^-\cdot 2CH_2Cl_2$ ($5^+I_5^-\cdot 2CH_2Cl_2$). The molecular and electronic structures of **1**–**4**, **6**, 1^+, and 5^+ were established by different spectra, single-crystal X-ray bond parameters, cyclic voltammetry, and DFT calculations.

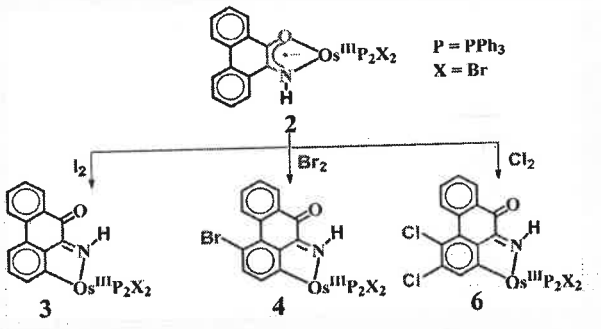

INTRODUCTION

The coordination chemistry of redox-noninnocent ligands is enthralling because of the participation of these ligands in various types of intra- and intermolecular redox reactions via the coordinated metal ions.[1] Moreover, the spectral features, valence tautomerism, and catalytic activities of these complexes have attracted researchers to develop functional materials based on the redox-noninnocent fragments.[2] In this regard, the coordination chemistry of catechol,[3] *o*-aminophenol,[4] and *o*-phenylenediamine[5] developed noticeably and the redox chemistry of these molecules is reviving many sections of chemical science. In many instances the chemistry of *o*-aminophenol derivatives supersedes that of catechol, as the valence of N is higher than that of O, opening up a scope in the design of ligands that contain multiple redox centers.[6] However, the reported coordination and redox chemistry of 9,10-phenanthreneiminoquinone (PIQ), which is an analogue of *o*-iminobenzosemiquinone, is limited and only one complex of ruthenium ion has been documented so far.[7] In this work, we explore the coordination and redox chemistry of PIQ with osmium ion. Reduction of PIQ by a hydridoosmium(II) precursor affording a 9,10-phenanthreneiminoquinonate anion radical ($PIQ^{\bullet-}$) complex of osmium(II) is authenticated. The search envisaged that PIQ is an ambidentate[8] redox-noninnocent ligand toward a heavier transition-metal ion, giving a new route to the creation of M–Ar bonds.[9] Oxidation of $PIQ^{\bullet-}$ complexes of osmium(III) by X_2 (X = I, Br, Cl) or by coulometry activates an aromatic C–H bond adjacent to the imine function, promoting an ortho-metalation reaction as depicted in Chart 1.

The synergic conversions of *o*-iminobenzosemiquione to *o*-iminobenzoquinone and N,O-chelate to N,C-chelate have not been observed in the vast coordination and redox chemistry of

Received: January 7, 2016
Published: May 5, 2016

DOI: 10.1021/acs.inorgchem.6b00040
Inorg. Chem. 2016, 55, 4746–4756

Chart 1

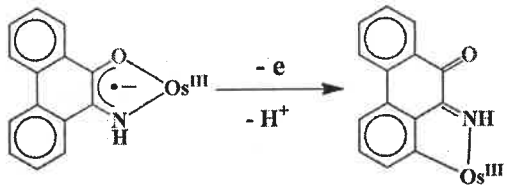

o-aminophenols of transition-metal ions. It is noted that, in a similar type of reaction with the 9,10-phenanthrenequinone platform, no ortho-metalation reaction was established. In this article, $PIQ^{\bullet-}$ complexes of osmium(II/III) of types *trans*-$[Os^{II}(PIQ^{\bullet-})(PPh_3)_2(CO)Br]$ (**1**) and *trans*-$[Os^{III}(PIQ^{\bullet-})(PPh_3)_2Br_2]$ (**2**) are reported. The trans abbreviation of the complexes is because of the two PPh_3 ligands which reside trans to each other. Oxidation of **1** by I_2 gave a $PIQ^{\bullet-}$ complex of osmium(III) of the type *trans*-$[Os^{III}(PIQ^{\bullet-})(PPh_3)_2(CO)Br]^+1/2I_3^-1/2Br^-$ ($\mathbf{1}^+1/2I_3^-1/2Br^-$), while oxidation of **2** with halogens generated PIQ complexes that contain an Os^{III}–Ar bond. The reaction of **2** with I_2 afforded an ortho-metalated derivative of the type *trans*-$[Os^{III}(C,N\text{-}PIQ)(PPh_3)_2Br_2]\cdot 2CH_2Cl_2$ ($\mathbf{3}\cdot 2CH_2Cl_2$) in moderate yields (C,N-PIQ = ortho-metalated PIQ). The reaction of **2** with Br_2 proceeds with ortho-metalation and monobromination of the aromatic ring, generating *trans*-$[Os^{III}(C,N\text{-}PIQ^{Br})(PPh_3)_2Br_2]\cdot 2CH_2Cl_2$ ($\mathbf{4}\cdot 2CH_2Cl_2$), where $C,N\text{-}PIQ^{Br}$ is a ortho-metalated 4-bromo PIQ, while the reaction with Cl_2 promotes ortho metalation and dichlorination of the aromatic ring, generating *trans*-$[Os^{III}(C,N\text{-}PIQ^{Cl2})(PPh_3)_2Br_2]$ (**6**), where $C,N\text{-}PIQ^{Cl2}$ is an ortho-metalated 3,4-dichloro PIQ, as depicted in Chart 2. For comparison, a similar reaction of I_2 with the 9,10-phenanthrenequinone (PQ) analogue of **2**, *trans*-$[Os^{III}(PQ^{\bullet-})(PPh_3)_2Br_2]$ ($\mathbf{2}_{PQ}$),[10] does not promote any ortho-metalation reaction and furnishes only a PQ complex of the type *trans*-$[Os^{III}(PQ)(PPh_3)_2Br_2]^+I_5^-$ ($\mathbf{5}^+I_5^-$). **1**–**4**, **6**, $\mathbf{1}^+I_3^-$, and $\mathbf{5}^+I_5^-$ were substantiated by different spectra, cyclic voltammetry, spectroelectrochemical measurements, single-crystal X-ray structure determinations, and density functional theory (DFT) calculations.

EXPERIMENTAL SECTION

Materials and Physical Measurements. Reagents or analytical-grade materials were obtained from commercial suppliers and used without further purification. The precursors $[Os^{II}(PPh_3)_3(CO)(H)Br]$[11] and $[Os^{II}(PPh_3)_3Br_2]$ were prepared by reported procedures.[11] Spectroscopic-grade solvents were used for spectroscopic and electrochemical measurements. The C, H, and N contents of the compounds were obtained from a PerkinElmer 2400 Series II elemental analyzer. The elemental analyses were performed after evaporating the solvents under high vacuum. Infrared spectra of the samples were measured from 4000 to 400 cm^{-1} with KBr pellets at 295 K on a PerkinElmer Spectrum RX 1 Fourier transform infrared (FT-IR) spectrophotometer. ^1H NMR spectra in $CDCl_3$ were recorded on a Bruker DPX 300 MHz spectrometer. Electrospray ionization (ESI) mass spectra were recorded on a micro mass Q-TOF mass spectrometer. Electronic absorption spectra of solutions of the complexes were recorded on a PerkinElmer Lambda 750 spectrophotometer in the range 3300–175 nm. The X-band EPR spectra were recorded on a Magnettech GmbH MiniScope MS400 spectrometer (equipped with TC H03 temperature controller), where the microwave frequency was measured with an FC400 frequency counter. The EPR spectra were simulated using EasySpin software. The electroanalytical instrument BASi Epsilon-EC for cyclic voltammetric experiments in CH_2Cl_2 containing 0.2 M tetrabutylammonium hexafluorophosphate as supporting electrolyte was used. A BASi platinum working electrode, platinum auxiliary electrode, and Ag/AgCl reference electrode were used for the measurements. The redox potential data were referenced versus the ferrocenium/ferrocene, Fc^+/Fc, couple. A BASi SEC-C thin-layer quartz glass spectroelectrochemical cell kit (light path length of 1 mm) with platinum gauze working electrode and SEC-C platinum counter electrode was used for spectroelectrochemistry measurements. All of the physicochemical data were collected on the isolated complexes *trans*-$[Os^{II}(PIQ^{\bullet-})(PPh_3)_2(CO)Br]$ (**1**), *trans*-$[Os^{III}(PIQ^{\bullet-})(PPh_3)_2(CO)Br]^+1/2I_3^-1/2Br^-$ ($\mathbf{1}^+1/2I_3^-1/2Br^-$), *trans*-$[Os^{III}(PIQ^{\bullet-})(PPh_3)_2Br_2]$ (**2**), *trans*-$[Os^{III}(C,N\text{-}PIQ)(PPh_3)_2Br_2]\cdot 2CH_2Cl_2$ ($\mathbf{3}\cdot 2CH_2Cl_2$), *trans*-$[Os^{III}(C,N\text{-}PIQ^{Br})(PPh_3)_2Br_2]\cdot 2CH_2Cl_2$ ($\mathbf{4}\cdot 2CH_2Cl_2$), *trans*-$[Os^{III}(C,N\text{-}PIQ^{Cl2})(PPh_3)_2Br_2]$ (**6**), and *trans*-$[Os^{III}(PQ)(PPh_3)_2Br_2]^+I_5^-\cdot 2CH_2Cl_2$ ($\mathbf{5}^+I_5^-\cdot 2CH_2Cl_2$).

Syntheses. *9,10-Phenanthreneiminoquinone (PIQ).* PIQ was synthesized by a reported procedure.[12]

trans-$[Os^{II}(PIQ^{\bullet-})(PPh_3)_2(CO)Br]$ (1). To a solution of PIQ in toluene (30 mL) was added $[Os^{II}(PPh_3)_3(CO)(H)Br]$ (100 mg, 0.1 mmol) under argon, and the solution was refluxed with stirring at 373 K for 1 h. A dark brown solid of **1** separated out, which was filtered, dried in air, and collected. Yield: 65 mg (66% with respect to osmium). Single crystals for X-ray analyses and spectroscopic and electrochemical measurements were prepared by slow diffusion of *n*-hexane into a CH_2Cl_2 solution of **1** in a glass tube at 295 K. Mass spectral data [electrospray ionization (ESI) positive ion, CH_2Cl_2]: *m/z* 1029 for $[\mathbf{1}]^+$. Anal. Calcd for $C_{51}H_{39}BrNO_2P_2Os$: C, 59.47; H, 3.82; N, 1.36. Found: C, 59.23; H, 3.80; N, 1.36. IR/cm^{-1} (KBr): ν 3389 (br), 3052 (m), 1909 (s), 1602 (m), 1581 (m), 1523 (m), 1482 (m), 1433 (s), 1363 (s), 1316 (s), 1096 (s), 731 (m), 707 (s), 693 (s), 512 (s).

trans-$[Os^{III}(PIQ^{\bullet-})(PPh_3)_2(CO)Br]^+1/2I_3^-1/2Br^-$ ($\mathbf{1}^+1/2I_3^-1/2Br^-$). To a CH_2Cl_2 solution (10 mL) of **1** (50 mg, 0.05 mmol) was added an iodine (20 mg, 0.075 mmol) solution in *n*-hexane (10 mL), and it was allowed to diffuse at 295 K. After a few days, black crystals of $\mathbf{1}^+1/2I_3^-1/2Br^-$ separated out, which were filtered and dried in air.

Chart 2. Isolated $PIQ^{\bullet-}$ (**1**, $\mathbf{1}^+$, and **2**), PIQ (**3**, **4**, and **6**), PQ ($\mathbf{5}^+$), and $PQ^{\bullet-}$ ($\mathbf{2}_{PQ}$) Complexes

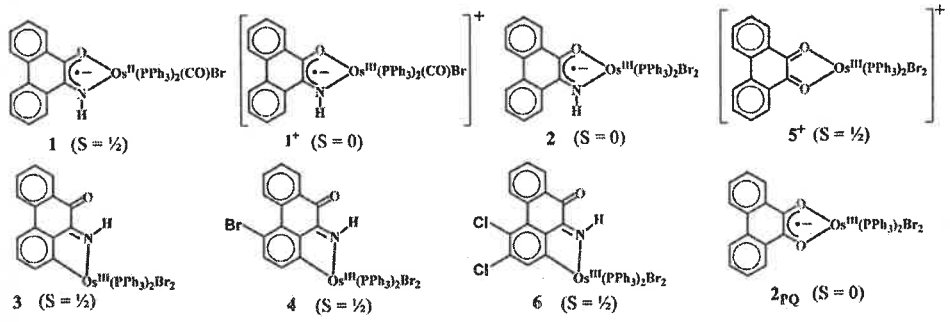

DOI: 10.1021/acs.inorgchem.6b00040
Inorg. Chem. 2016, 55, 4746–4756

Yield: 40 mg (~54% with respect to osmium). The product was used for single-crystal X-ray structure determination and spectroscopic and electrochemical measurements. It is proposed that the partial decomposition of **1** during the oxidation produces the Br^- ion which partially occupies (occupation factor 0.5) the lattice of $1^+1/2I_3^-1/2Br^-$. Mass (ESI, positive ion, CH_2Cl_2): m/z 1029 for $[1]^+$. Anal. Calcd for $C_{51}H_{39}Br_{1.5}I_{1.5}NO_2P_2Os$: C, 48.61; H, 3.12; N, 1.11. Found: C, 48.43; H, 3.11; N, 1.11. ^1H NMR ($CDCl_3$, 300 MHz): δ (ppm) 13.40 (1H, s), 8.45 (1H, d), 8.28 (1H, d), 8.20 (1H, d), 7.97 (1H, t), 7.67 (1H, t), 7.53–7.47 (8H, m), 7.30–7.21 (25H, m). IR/cm^{-1} (KBr): ν 3431 (br), 3050 (w), 1998 (s), 1601 (m), 1433 (m), 1385 (s), 1317 (m), 1094 (s), 750 (m), 696 (s), 521 (s).

trans-[Os^{III}(PIQ$^{\bullet-}$)(PPh_3)$_2Br_2$] (2). To a solution of PIQ in toluene (30 mL) was added $[Os^{II}(PPh_3)_3Br_2]$ (115 mg, 0.1 mmol) under argon, and the solution was refluxed with stirring at 373 K for 1 h. A dark red solid of **2** separated out, which was filtered and dried in air. Yield: 60 mg (~55% with respect to osmium). Single crystals of **2** were prepared by slow diffusion of *n*-hexane into the CH_2Cl_2 solution of **2** in a glass tube at 295 K for X-ray analyses and spectroscopic and electrochemical measurements. Mass spectral data [electrospray ionization (ESI) positive ion, CH_2Cl_2]: m/z 1081 for $[2]^+$. Anal. Calcd for $C_{50}H_{39}Br_2NOP_2Os$: C, 55.51; H, 3.63; N, 1.29. Found: C, 55.33; H, 3.61; N, 1.29. ^1H NMR ($CDCl_3$, 300 MHz): δ (ppm) 12.7 (1H, s), 8.81 (2H, d), 8.07 (2H, t), 7.93 (2H, d), 7.81 (2H, d), 7.63–7.53 (15H, m), 7.45 (4H, d), 7.26–7.16 (11H, m). IR/cm^{-1} (KBr): ν 3448 (br), 3054 (m), 1601 (m), 1497 (m), 1482 (m), 1434 (s), 1375 (m), 1353 (m), 1316 (s), 1094 (s), 746 (s), 693 (s), 512 (s).

trans-[Os^{III}(C,N-PIQ)(PPh_3)$_2Br_2$]·2CH_2Cl_2 (3·2CH_2Cl_2). To a CH_2Cl_2 (5 mL) solution of complex **2** (50 mg, 0.05 mmol) was added an iodine (20 mg, 0.075 mmol) solution in *n*-hexane. The resulting solution was allowed to diffuse at 295 K. After a few days dark reddish brown crystals of 3·2CH_2Cl_2 separated out, which were filtered and dried in air. These crystals were used for single-crystal X-ray diffraction studies and spectroscopic and electrochemical measurements. Yield: 40 mg (~43% with respect to osmium). Mass spectral data [electrospray ionization (ESI), positive ion, CH_2Cl_2]: m/z 1001 for $[3 - Br]^+$. Anal. Calcd for $C_{50}H_{38}Br_2NOP_2Os$: C, 55.56; H, 3.54; N, 1.30. Found: C, 55.36; H, 3.52; N, 1.30. IR/cm^{-1} (KBr): ν 3435 (br), 3053 (w), 1637 (m), 1596 (s), 1480 (m), 1432 (m), 1347 (s), 1315 (m), 1093 (s), 750 (s), 693 (s), 520 (s).

trans-[Os^{III}(C,N-PIQ^{Br})(PPh_3)$_2Br_2$]·2CH_2Cl_2 (4·2CH_2Cl_2). To a CH_2Cl_2 (5 mL) solution of **2** (50 mg, 0.05 mmol) was added bromine (1 drop). The mixture was stirred for 10 min in air. Bromine (1 drop) in *n*-hexane was further added slowly to the resulting CH_2Cl_2 solution and was allowed to diffuse at 295 K. After a few days dark red crystals of 4·2CH_2Cl_2 separated, which were filtered and dried in air. This crop was used for the single-crystal X-ray diffraction studies and all spectroscopic and electrochemical measurements. Yield: 20 mg (~27% with respect to osmium). Mass spectral data [electrospray ionization (ESI), positive ion, CH_2Cl_2]: m/z 1082 for $[4 - Br]^+$. Anal. Calcd for $C_{50}H_{37}Br_3NOP_2Os$: C, 51.78; H, 3.22; N, 1.21. Found: C, 51.46; H, 3.21; N, 1.21. IR/cm^{-1} (KBr): ν 3435 (br), 3053 (w), 1642 (m), 1597 (s), 1481 (m), 1435 (m), 1374 (s), 1304 (m), 1092 (s), 748 (s), 696 (s), 525 (s).

trans-[Os^{III}(C,N-PIQ^{Cl2})(PPh_3)$_2Br_2$] (6). To a CH_2Cl_2 (5 mL) solution of **2** (50 mg, 0.05 mmol) was passed dry Cl_2 gas for 1 min. The mixture was stirred for 20 min in air. *n*-Hexane was further added slowly to the resulting CH_2Cl_2 solution and was allowed to diffuse at 295 K. After a few days crystals of **6** separated, which were filtered and dried in air. This crop was used for the single-crystal X-ray diffraction studies and all spectroscopic and electrochemical measurements. Yield: 20 mg (~27% with respect to osmium). Mass spectral data [electrospray ionization (ESI), positive ion, CH_2Cl_2]: m/z 1069 for $[6 - Br]^+$. Anal. Calcd for $C_{50}H_{36}Cl_2Br_2NOP_2Os$: C, 52.23; H, 3.16; N, 1.22. Found: C, 51.99; H, 3.15; N, 1.22. IR/cm^{-1} (KBr): ν 3275 (m), 3057 (m), 1655 (s), 1591 (s), 1528 (s), 1481 (s), 1469 (s), 1434 (s), 1283 (s), 1187 (m), 1151 (m), 1091 (s), 743 (s), 694 (s), 519 (s).

Caution! Since Br_2 vapor and Cl_2 gas are hazardous oxidizing gases with an irritating odor and are extremely toxic by inhalation, caution is advised, and handling of only a small quantity is recommended.

trans-[Os^{III}(PQ)(PPh_3)$_2Br_2$]$^+I_5^-$·2CH_2Cl_2 ($5^+I_5^-$·2CH_2Cl_2). To a CH_2Cl_2 solution (5 mL) of $[Os^{III}(PQ^-)(PPh_3)_2Br_2]$ (2_{PQ})[10] (50 mg, 0.05 mmol) was added an iodine (20 mg, 0.075 mmol) solution in *n*-hexane (10 mL), and it was allowed to diffuse at 295 K. After a few days, black crystals of $5^+I_5^-$·2CH_2Cl_2 separated out, which were filtered and dried in air. Yield: 35 mg (~54% with respect to osmium). Single-crystal X-ray structure determination and all spectroscopic and electrochemical measurements were done using the product. Mass (ESI, positive ion, CH_2Cl_2): m/z 1082 for $[5]^+$. Anal. Calcd for $C_{50}H_{38}Br_2I_5O_2P_2Os$: C, 34.97; H, 2.23. Found: C, 33.88; H, 2.22. IR/cm^{-1} (KBr): ν 1639 (m), 1593 (s), 1479 (s), 1445 (s), 1432 (s), 1355 (s), 1303 (s), 1092 (s), 745 (s), 691 (s), 518 (s).

Single-Crystal X-ray Structure Determinations of the Complexes. Dark single crystals of *trans*-$[Os^{II}(PIQ^-)(PPh_3)_2(CO)Br]$ (**1**), *trans*-$[Os^{III}(PIQ^{\bullet-})(PPh_3)_2(CO)Br]^+1/2I_3^-1/2Br^-$ ($1^+1/2I_3^-1/2Br^-$), *trans*-$[Os^{III}(PIQ^{\bullet-})(PPh_3)_2Br_2]$ (**2**), *trans*-$[Os^{III}$(C,N-PIQ)$(PPh_3)_2Br_2]$·2CH_2Cl_2 (3·2CH_2Cl_2), *trans*-$[Os^{III}$(C,N-PIQ^{Br})-$(PPh_3)_2Br_2]$·2CH_2Cl_2 (4·2CH_2Cl_2), *trans*-$[Os^{III}$(C,N-PIQ^{Cl2})-$(PPh_3)_2Br_2]$ (**6**) and *trans*-$[Os^{III}(PQ)(PPh_3)_2Br_2]^+I_5^-$·2$CH_2Cl_2$ ($5^+I_5^-$·2CH_2Cl_2) were picked up with nylon loops and mounted on Bruker APEX-II CCD and Bruker AXS D8 QUEST ECO diffractometers equipped with a Mo-target rotating-anode X-ray source and a graphite monochromator (Mo Kα, λ = 0.71073 Å). Final cell constants were obtained from least-squares fits of all measured reflections. Intensity data were corrected for absorption using intensities of redundant reflections. The structures were readily solved by direct methods and subsequent difference Fourier techniques. The crystallographic data of **1**, $1^+1/2I_3^-1/2Br^-$, **2**, 3·2CH_2Cl_2, 4·2CH_2Cl_2, **6**, and $5^+I_5^-$·2CH_2Cl_2 are given in Table S1 in the Supporting Information. The Siemens SHELXS-97[13a] software package was used for structure solution, SHELXL-97[13b] was used for the refinement, and XS version 2013/1,[13c] XT version 2014/4,[13d] and XL version 2014/7[13e] were used for the structure solution and refinement. All non-hydrogen atoms were refined anisotropically. Hydrogen atoms were placed at calculated positions and refined as riding atoms with isotropic displacement parameters. All the A and B level errors of the checkcif files of the complexes are due to the disordered solvents or anions. The checkcif file of $1^+1/2I_3^-1/2Br^-$ exhibits an A level error due to a calculated residual density of 4.10 eV^{-3}; this may correspond to an unaccounted disordered anion which is insignificant. The B level errors due to residual densities at the coordination sphere of $1^+1/2I_3^-1/2Br^-$ and 4·2CH_2Cl_2 are because of the diffuse osmium d orbital, while the B level error of **2** due to a solvent void originates from the evaporation of the volatile solvent from the stable lattice.

Density Functional Theory Calculations. All calculations reported in this article were done with the Gaussian 03W[14] program package supported by GaussView 4.1. The DFT[15] and time-dependent (TD) DFT[16] calculations were performed at the level of the Becke three-parameter hybrid functional with the nonlocal correlation functional of Lee, Yang, and Parr (B3LYP).[17] Gas-phase geometries of *trans*-$[Os^{II}(PIQ^{\bullet-})(PMe_3)_2(CO)Br]$ (1^{Me}), *trans*-$[Os^{III}(PIQ)$-$(PMe_3)_2Br_2]^+$ (2^{Me+}), *trans*-$[Os^{III}(PIQ^{2-})(PMe_3)_2Br_2]^-$ (2^{Me-}), and *trans*-$[Os^{III}$(C,N-PIQ)$(PMe_3)_2Br_2]$ (3^{Me}) were optimized with a doublet spin state, using Pulay's direct inversion[18] in the iterative subspace (DIIS), "tight" convergent self-consistent field procedure[19] ignoring symmetry. Similarly, *trans*-$[Os^{III}(PIQ^{\bullet-})(PMe_3)_2(CO)Br]^+$ (1^{Me+}) and *trans*-$[Os^{III}(PIQ^{\bullet-})(PMe_3)_2Br_2]$ (2^{Me}, CSS, Triplet, and OSS) were optimized with a singlet spin state. In all calculations, a LANL2DZ basis set along with the corresponding effective core potential (ECP) was used for osmium.[20] A valence double-ζ basis set, 6-31G, was used for H.[21] For non-hydrogen atoms C, N, P, and Br a valence double-ζ basis set with diffuse and polarization functions, 6-31++G**,[22] was employed for all calculations. The 60 lowest singlet excitation energies on each of the optimized geometries of 1^{Me}, 2^{Me}, and 3^{Me} were elucidated by TD DFT calculations.

DOI: 10.1021/acs.inorgchem.6b00040
Inorg. Chem. 2016, 55, 4746–4756

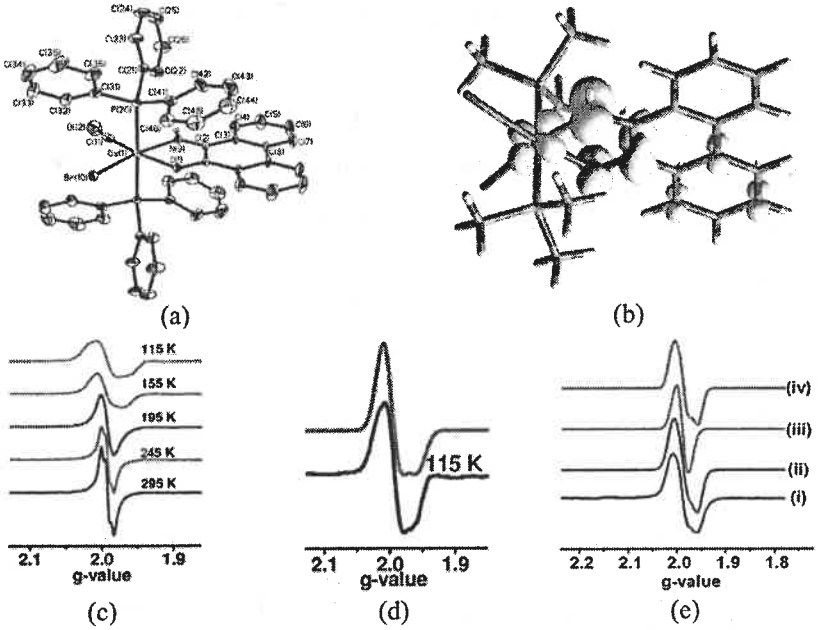

Figure 1. (a) Molecular geometry of **1** in the crystal form (40% thermal ellipsoids; H atoms omitted for clarity), (b) Atomic spin density plot of 1^{Me} obtained from Mulliken spin population analysis (Os1, 0.14; O1A, 0.14; N9, 0.39; C2A, 0.21; C2, −0.01). (c) Variable-temperature (295−115 K) X-band EPR spectra of **1** in CH_2Cl_2. (d) Simulated EPR spectrum of **1** at 115 K. (e) Simulated EPR spectra of a powder of **1** at 295 K.

RESULTS AND DISCUSSION

Syntheses and Characterization. PIQ was synthesized by a reported procedure.[12] The PIQ complexes isolated in this work are given in Chart 2. All of the complexes have a trans geometry with respect to two PPh_3 ligands. The reaction of PIQ with $[Os^{II}(PPh_3)_3(CO)(H)Br]$ in boiling toluene affords **1**, while the reaction of PIQ with $[Os^{II}(PPh_3)_3Br_2]$ generates **2** in good yield. In both cases PIQ is reduced to $PIQ^{\bullet-}$; in the former case hydridoosmium(II) is the reducing equivalent, while in the case of **2** osmium(II) is oxidized to osmium(III) ion, reducing PIQ to the $PIQ^{\bullet-}$ state. It is noted that the I_2 molecule reacts differently with **1** and **2**. The reaction of **1** in CH_2Cl_2/*n*-hexane with I_2 produced $1^+1/2I_3^-1/2Br^-$, while the reaction of **2** with I_2 progresses with an ortho-metalation reaction, affording **3** in good yields. However, the reactions of **2** with Br_2 and Cl_2 promote ortho metalation and halogenations of the aromatic ring, producing **4** and **6**. Oxidation of the $[Os^{III}(PIQ^{\bullet-})]$ state activates the aromatic C−H bond adjacent to the imine function, promoting ortho metalation of PIQ. This is an ortho-metalation reaction induced by iminosemiquinone to iminoquinone conversion. Notably, constant-potential coulometric oxidation of **2** at +0.35 V generates *trans*-$[Os^{III}(PIQ)(PPh_3)_2Br_2]^+$ (2^+), which is not stable in solution and slowly converts to **3**, and a part hydrolyzes to a PQ complex of the type *trans*-$[Os^{III}(PQ^{\bullet-})(PPh_3)_2Br_2]$ (2_{PQ}), reported recently. Changes in the UV/vis absorption spectrum of 2^+ ion in CH_2Cl_2 were recorded over an interval of about 24 h and are illustrated in Figure S1a in the Supporting Information. After 10 days the electrolyzed solution containing 2^+ ion and tetrabutylammonium hexafluorophosphate as an electrolyte was evaporated to dryness under vacuum and the contents were purified on a silica gel column. Elution with a 1/2 CH_2Cl_2/*n*-hexane solvent mixture afforded green 2_{PQ} and elution with a 4/1 solvent mixture yielded **2**, while elution with a 4/1 CH_2Cl_2/acetonitrile solvent mixture gave **3** in lower yields (another part was adsorbed on the silica surface); all of these compounds were analyzed by UV/vis and IR spectra and cyclic voltammetry. For comparison, the UV/vis absorption spectra of these products are illustrated in Figure S1b. The study authenticated that 2^+ ion in the absence of halogens also furnishes an ortho-metalated derivative. 2_{PQ} reacts differently with I_2 solution, affording $5^+I_5^-$, where no ortho-metalation reaction is observed. Details of the syntheses of the complexes are outlined in the Experimental Section. The complexes were characterized by elemental analyses and mass, IR, and ^1H NMR spectra. The data are given in the Experimental Section. The N−H stretching frequencies span a range of 3390−3450 cm^{-1}. The $\nu_{C\equiv O}$ bands of **3**, **4**, and $5^+I_5^-$ appear at 1637−1642 cm^{-1}, while those of **1**, $1^+I_3^-$, and **2** are observed at 1480−1433 cm^{-1}. The difference in the $\nu_{C\equiv O}$ bands of **1** (1909 cm^{-1}) and $1^+1/2I_3^-1/2Br^-$ (1998 cm^{-1}) is relatively higher than that of 1_{PQ} (1909 cm^{-1}) and 1_{PQ}^+ (1955 cm^{-1}).[10] This is due to the conversion of osmium(II) of **1** to osmium(III) in the 1^+ ion having weaker $d_\pi \rightarrow \pi_{C\equiv O}^*$ back-bonding.

Assignment of the Electronic States of the Complexes. The electronic structures of the complexes were elucidated by the bond parameters obtained from the single-crystal X-ray structure determinations, EPR spectra, and atomic spin population analyses. The crystallographic data of **1**, $1^+1/2I_3^-1/2Br^-$, **2**, $3{\cdot}2CH_2Cl_2$, $4{\cdot}2CH_2Cl_2$, **6**, and $5^+I_5^-{\cdot}2CH_2Cl_2$ are summarized in Table S1 in the Supporting Information. Density functional theory (DFT) calculations were employed for the PMe_3 analogues to predict the atomic spin densities in the complexes. The gas-phase geometries of *trans*-$[Os^{II}(PIQ)(PMe_3)_2(CO)Br]^+$ (1^{Me+}) and *trans*-$[Os^{III}(PIQ^{\bullet-})(PMe_3)_2Br_2]$ (2^{Me}) were optimized with a singlet spin state, while the geometries of *trans*-$[Os^{II}(PIQ^{\bullet-})(PMe_3)_2(CO)Br]$ (1^{Me}), *trans*-$[Os^{III}(PIQ)(PMe_3)_2Br_2]^+$ (2^{Me+}), *trans*-$[Os^{III}(PIQ^{2-})(PMe_3)_2Br_2]^-$ (2^{Me-}), and *trans*-$[Os^{III}(C,N\text{-}PIQ)(PMe_3)_2Br_2]$ (3^{Me}) were optimized with a doublet spin state; optimized

DOI: 10.1021/acs.inorgchem.6b00040
Inorg. Chem. 2016, 55, 4746−4756

Table 1. Selected Experimental Bond Lengths (Å) of 1, $1^+1/2I_3^-1/2Br^-$, 2, $3{\cdot}2CH_2Cl_2$, $4{\cdot}2CH_2Cl_2$, $5^+I_5^-{\cdot}2CH_2Cl_2$, and 6

bond	1	$1^+1/2I_3^-1/2Br^-$	2	$3{\cdot}2CH_2Cl_2$	$4{\cdot}2CH_2Cl_2$	$5^+I_5^-{\cdot}2CH_2Cl_2$	6
Os–O		2.153(2)				2.028(6)	
Os–N		1.981(3)		2.025(2)	2.018(4)		2.017(9)
Os–O/N	2.079(2)		2.006(3)				
Os–PPh_3	2.396(3)	2.412(3)	2.404(2)	2.391(2)	2.415(2)	2.422(2)	2.403(3)
	2.396(3)	2.417(3)	2.404(2)	2.418(3)	2.407(3)	2.429(2)	2.417(3)
Os–Br	2.556(4)	2.609(1)	2.514(2)	2.502(1)	2.490(2)	2.436(3)	2.4546(16)
			2.514(2)	2.584(1)	2.552(2)	2.457(3)	2.5617(15)
Os-CO	1.878(14)	1.859(3)					
Os–C				2.059(3)	2.044(5)		2.060(11)
C–O		1.274(4)		1.223(4)	1.221(6)	1.247(11)/ 1.270(10)	1.181(17)
C–N		1.311(4)		1.298(4)	1.296(5)		1.271(15)
C–O/N	1.288(4)		1.307(4)				
C–C (chelate)	1.440(7)	1.452(4)	1.402(9)	1.484(4)	1.481(6)	1.454(12)	1.518(16)

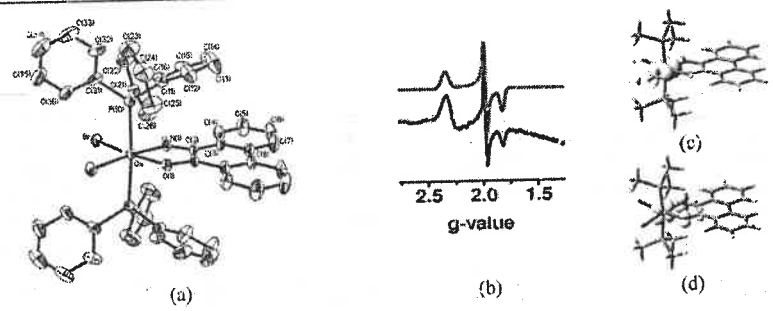

Figure 2. (a) Molecular geometry of 2 in the crystal form (40% thermal ellipsoids; H atoms omitted for clarity). (b) X-band EPR spectra of 2^- at 115 K (black, experimental; red, simulated). Atomic spin density plots of (c) 2^{Me+} (Os, 0.93) and (d) 2^{Me-} (Os, 0.45; O1, 0.11; N1, 0.30; C2A, 0.12; C2, −0.07) obtained from Mulliken spin population analyses.

coordinates are given in Tables S5–S10 in the Supporting Information.

1 crystallizes in the space group $C2/c$. The molecular structure of 1 in the crystal form and the atom labeling schemes are illustrated in Figure 1a. The molecule exhibits a crystallographic disorder along a C_2 axis which bisects the PIQ fragment. Thus, (CO, Br) and (N9, O1) pairs are crystallograpically equivalent. The diffraction study only provides us the average of the Os–O/N and C–O/N lengths, as summarized in Table 1. The average Os–O/N lengths are 2.079(2) Å. The average C–O/N lengths, 1.288(4) Å, are relatively longer and are similar to those of $PIQ^{\bullet-}$ coordinated to ruthenium(II/III) ions isolated recently. The C–C length of the N,O-chelate, 1.440(7) Å, is relatively shorter than those of a neutral PIQ complex of ruthenium(III) ion.[23] The C–C length of the chelate correlates well to that of the $PQ^{\bullet-}$ in *trans*-$[Os^{II}(PQ^{\bullet-})(PPh_3)_2(CO)Br]$ (1_{PQ}) and 2_{PQ}.[10] Thus, the bond parameters of the N,O-chelate imply that 1 is a $PIQ^{\bullet-}$ complex of osmium(II) ion.

The X-band EPR spectra of a powder, solution, and frozen glass of 1 were recorded, and the measurement parameters are summarized in Table S2 in the Supporting Information. The isotropic signal of a CH_2Cl_2 solution of 1, which exhibits hyperfine splitting due to ^{14}N and ^1H nuclei, is illustrated in Figure 1c. The g value obtained from a simulation of the spectrum, 1.993 (A_N = 9.7 G; A_H = 10.8 G), is consistent with the existence of $PIQ^{\bullet-}$ in 1. Generally organic radicals exhibit an EPR signal at g = 2.00 ± 0.01.[10] The anisotropic EPR spectrum of the CH_2Cl_2 frozen glass at 115 K (Figure 1c) is relatively broader (g_1 = 1.958; g_2 = 2.004; g_3 = 2.008; Δg = 0.05), which was simulated by considering an approximately axial spectrum. This indicates that, in the frozen glass, the contribution of the *trans*-$[Os^{III}(PIQ^{2-})(PPh_3)_2(CO)Br]$ state to the ground electronic state is significant. Variable-temperature (295–115 K) EPR spectra of 1 confirmed that with a decrease of temperature the contribution of the $[Os^{III}(PIQ^{2-})]$ state increases and the anisotropicity of the spectra increases. The phenomenon predicts the existence of a temperature-dependent tautomeric equilibrium of the type $[Os^{II}(PIQ^{\bullet-})] \leftrightharpoons [Os^{III}(PIQ^{2-})]$ in a solution of 1. It is noteworthy that the EPR signal of the powder sample of 1 at 295 K is similar to that of the frozen glass, as depicted in Figure 1c, and the spectrum was simulated considering the coexistence of $[Os^{II}(PIQ^{\bullet-})]$ and $[Os^{III}(PIQ^{2-})]$ states in the solid state. The spectrum (ii) was produced considering the $[Os^{III}(PIQ^{2-})]$ (g_1 = 1.958, g_2 = 1.990, and g_3 = 2.012) state and (iii) was obtained considering only the $[Os^{II}(PIQ^{\bullet-})]$ (g = 1.991) state, while the spectrum (iv) was achieved having 1/1 contributions of these two radical and non-radical states.

The $PIQ^{\bullet-}$ state in 1 is further authenticated by DFT calculations on 1^{Me}, the gas-phase geometry of which was optimized with a doublet spin state. The calculated bond parameters of 1^{Me} are similar to those obtained from an X-ray diffraction study of 1. The calculated bond parameters are summarized in Table S3 in the Supporting Information. The calculated average C–O/N lengths,1.329 Å, and the atomic spin density, which is heavily localized on the PIQ chelate as shown in Figure 1b, corroborate the reduction of PIQ to $PIQ^{\bullet-}$ coordinated to osmium(II) ion. It is noted that the spin scatters dominantly on the nitrogen atom (~39%), predicting a

DOI: 10.1021/acs.inorgchem.6b00040
Inorg. Chem. 2016, 55, 4746–4756

resonance form of type A as depicted in Scheme S1 in the Supporting Information. The localization of a small amount of spin (~14%) on one of the t_{2g} orbitals of osmium indicates a minor contribution of the $[Os^{III}(PIQ^{2-})]$ state in **1**, as predicted from the frozen-glass (115 K) and solid-state EPR spectra. The calculated coupling constants due to ^{14}N (I = 1) and ^{1}H (I = 1/2) nuclei, 8.6 and 9.8 G, are similar to those obtained experimentally.

2 crystallizes in the space group $C2/c$. The molecular structure of **2** in the crystal form and the atom-labeling schemes are illustrated in Figure 2a. Similar to the case for **1**, **2** exhibits crystallographic disorder along a C_2 axis which bisects the PIQ fragment. The average Os−O/N lengths, 2.006(3) Å, are relatively shorter than those of **1**. The average C−O/N lengths are relatively longer, 1.307(4) Å, while the C−C length of the chelate, 1.402(9) Å, is relatively shorter than those of the neutral PIQ coordinated to ruthenium(III) ion.[23] The relatively longer average C−O/N lengths of **2** in comparison to those of **1** can be explained by the inaccuracy of the diffraction study due to the disordered =O and =NH groups. The longer C−O/N bond lengths are consistent with the $PIQ^{\bullet-}$ state, and **2** is defined as a $PIQ^{\bullet-}$ complex of osmium(III). In contrast, the corresponding *o*-aminophenol analogue is a osmium(IV) complex of dianionic *o*-amidophenolate (AP^{2-}) of the type *trans*-$[Os^{IV}(AP^{2-})(PPh_3)_2Br_2]$.[24] Notably, in this coordination sphere, PQ and PIQ behave similarly and $\mathbf{2}_{PQ}$ is a $PQ^{\bullet-}$ complex of osmium(III).

The gas-phase geometry of $\mathbf{2}^{Me}$ was optimized with singlet and triplet spin states. The closed-shell singlet (CSS) solution of $\mathbf{2}^{Me}$ is stable, and the energies of the open-shell singlet (OSS) and the CSS solutions are exactly the same. However, the triplet solution is 9.48 kJ/mol higher in energy than the CSS solution. As the OSS solution did not converge to a lower energy, the calculated parameters of $\mathbf{2}^{Me}$ were not used for further analyses.

The X-band EPR spectra of the frozen CH_2Cl_2 glasses of $\mathbf{2}^{+}$ and $\mathbf{2}^{-}$ ions were recorded at 115 K, and the spectrum of $\mathbf{2}^{-}$ is depicted in Figure 2b, while the spectrum of $\mathbf{2}^{+}$ ion is shown in Figure S2b in the Supporting Information. The g parameters ($\mathbf{2}^{+}$, g_1 = 2.530, g_2 = 2.060, g_3 = 1.470, Δg = 1.06; $\mathbf{2}^{-}$in g_1 = 2.340, g_2 = 1.973, g_3 = 1.820, Δg = 0.52), obtained from simulation of the frozen-glass spectra, authenticated that the $\mathbf{2}^{+}$ and $\mathbf{2}^{-}$ ions are osmium(III) complexes of the types *trans*-$[Os^{III}(PIQ)(PPh_3)_2Br_2]^{+}$ and *trans*-$[Os^{III}(PIQ^{2-})(PPh_3)_2Br_2]^{-}$. The g values of some of the osmium(III) complexes[25] containing redox-innocent and -noninnocent ligands are as follows: $[Os\{S(CH_2Ph)_2\}_3Br_3]$, g_1 = 2.776, g_2 = 2.130, g_3 = 1.541; $[(pap)_2Os^{II}(\mu\text{-}L_2^{2-})Os^{III}(pap)_2]^{3+}$, g_1 = 2.032, g_2 = 1.964, g_3 = 1.842 (H_2L_2 = 1,4-diamino-9,10-anthraquinone, pap = 2-phenylazopyridine); $[Os(pap)_2(Q)]^{-}$, g_1 = 2.253, g_2 = 2.099, g_3 = 1.958, (Q = 4,6-di-*tert*-butyl-*N*-aryl-*o*-iminobenzoquinone; aryl = 3,5-dichlorophenyl); $[Os(L^a)_2]^{+}$, g_1 = 2.386, g_2 = 2.283, g_3 = 1.848, (HL^a = (2-[(2-*N*-phenylamino)phenylazo]-pyridine).

$\mathbf{2}^{Me+}$ and $\mathbf{2}^{Me-}$ were optimized with a doublet spin state. The calculated C−O and C−N lengths of $\mathbf{2}^{Me+}$, 1.281 and 1.326 Å (average C−O/N lengths, 1.303 Å), are relatively shorter than those of $\mathbf{2}^{Me}$, while these are 1.312 and 1.365 Å in the case of $\mathbf{2}^{Me-}$. In $\mathbf{2}^{Me+}$, the atomic spin is dominantly localized on the osmium ion (d_{xy} orbital) as depicted in Figure 2c, confirming that the $\mathbf{2}^{+}$ ion is an osmium(III) complex of neutral PIQ. To facilitate stronger d_{xz} (or d_{yz})→π_{PIQ}^{*} back-bonding, the d_{xy} orbital is singly occupied in the $\mathbf{2}^{+}$ ion. The relatively longer calculated C−O and C−N lengths (average C−O/N lengths, 1.338 Å) of $\mathbf{2}^{Me-}$ and the dispersion of atomic spin on both osmium ion (d_{xz} orbital) and the PIQ fragment as depicted in Figure 2d reveal the contributions of "$[Os^{III}(PIQ^{2-})]$" and "$[Os^{II}(PIQ^{\bullet-})]$" states to the ground electronic state of the $\mathbf{2}^{-}$ ion. The EPR spectrum correlates with a major contribution of the "$[Os^{III}(PIQ^{2-})]$" state to the $\mathbf{2}^{-}$ ion.

$\mathbf{1}^{+}1/2I_3^{-}1/2Br^{-}$ crystallizes in the space group $P\bar{1}$. The molecular structure of $\mathbf{1}^{+}1/2I_3^{-}1/2Br^{-}$ in the crystal form and the atom-labeling schemes are illustrated in Figure 3. The Os−O and Os−N lengths are 2.153(2) and 1.981(3) Å, respectively. The average C−O/N lengths is 1.293(4) Å. The C−C length is 1.452(4) Å. These bond parameters of the chelate are similar to those of **1** and **2**. This is consistent with the existence of $PIQ^{\bullet-}$ in the $\mathbf{1}^{+}$ ion, which is defined as a $PIQ^{\bullet-}$ complex of osmium(III) incorporating triphenylphosphine and carbonyl as coligands. This proposes that the I_2 molecule does not oxidize $PIQ^{\bullet-}$ of **1** to PIQ but rather oxidizes osmium(II) to osmium(III) ion. In contrast, the oxidation of the $PQ^{\bullet-}$ analogue of **1**, *trans*-$[Os^{II}(PQ^{\bullet-})(PPh_3)_2(CO)Br]$, by I_2 afforded a PQ complex of osmium(II) of the type *trans*-$[Os^{II}(PQ)(PPh_3)_2(CO)Br]^{+}I_3^{-}$.[10]

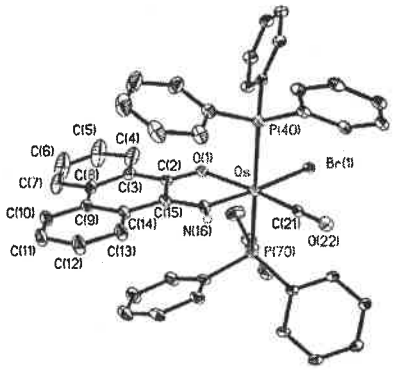

Figure 3. Molecular geometry of $\mathbf{1}^{+}1/2I_3^{-}1/2Br^{-}$ in the crystal form with 40% thermal ellipsoids (I_3, Br, and H omitted for clarity as applicable).

$\mathbf{3}\cdot 2CH_2Cl_2$ and $\mathbf{4}\cdot 2CH_2Cl_2$ crystallize in the space group $P2_1/c$, while **6** crystallizes in the space group $P2_12_12_1$. The molecular structures of $\mathbf{3}\cdot 2CH_2Cl_2$, $\mathbf{4}\cdot 2CH_2Cl_2$, and **6** in the crystal form and the atom-labeling schemes are illustrated in Figure 4. In comparison to those of **1**, $\mathbf{1}^{+}1/2I_3^{-}1/2Br^{-}$, and **2**, the C−O and C−N lengths of $\mathbf{3}\cdot 2CH_2Cl_2$, $\mathbf{4}\cdot 2CH_2Cl_2$, and **6** are relatively shorter, while the C−C lengths of the chelate are relatively longer. In these complexes, the average C−O/N lengths are 1.260(4), 1.259(6), and 1.226(17) Å and the C−C lengths are 1.484(4), 1.481(6), and 1.518(16) Å, respectively (Table 1). The Os^{III}−C lengths, 2.059(3), 2.044(5), and 2.017(9) Å in $\mathbf{3}\cdot 2CH_2Cl_2$, $\mathbf{4}\cdot 2CH_2Cl_2$, and **6** are relatively shorter than that, 2.105(16) Å, in *trans*-$[Os^{III}(DBQ)(PPh_3)_2Br_2]$ (DBQ = dibenzo[1,2]quinoxaline), while the Os^{III}−Br and Os^{III}−PPh_3 lengths of these complexes are approximately similar to those of the osmium(III) DBQ complex.[25] The calculated C−O and C−N lengths of $\mathbf{3}^{Me}$ with doublet spin state are 1.233 and 1.311 Å (average C−O/N lengths, 1.272 Å).

The EPR spectra of **3** and **4** are illustrated in Figure 5a,b. The g values obtained from simulation of the spectra are as follows: **3**, g_1 = 2.352, g_2 = 1.982, g_3 = 1.820; **4**, g_1 = 2.340, g_2 = 1.971, g_3

DOI: 10.1021/acs.inorgchem.6b00040
Inorg. Chem. 2016, 55, 4746−4756

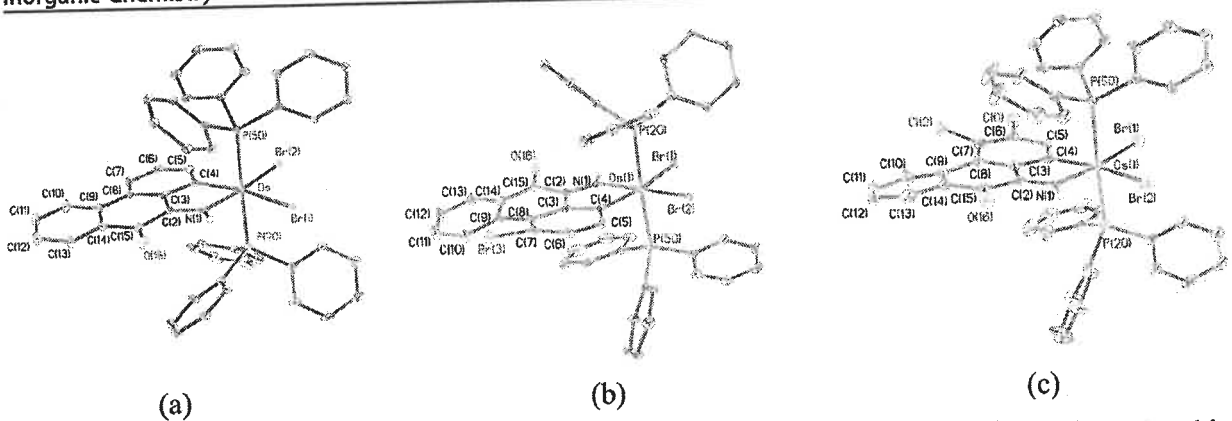

Figure 4. Molecular geometries of (a) $3{\cdot}2CH_2Cl_2$, (b) $4{\cdot}2CH_2Cl_2$, and (c) **6** in crystals with 40% thermal ellipsoids (CH_2Cl_2 and H omitted for clarity as applicable).

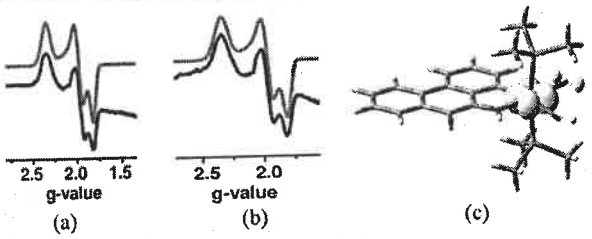

Figure 5. X-band EPR spectra of (a) **3** and (b) **4** in frozen CH_2Cl_2 glass (at 115 K; black, experimental; red, simulated). Atomic spin density plot of (c) 3^{Me} (Os, 0.95) obtained from Mulliken spin population analyses.

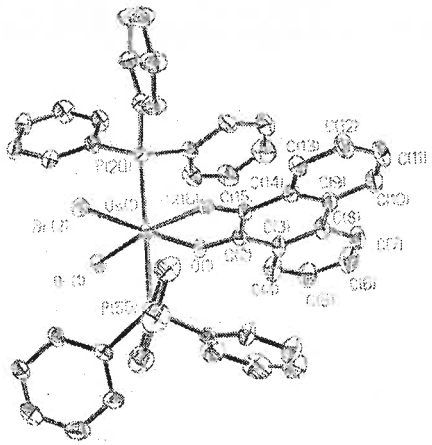

Figure 6. Molecular geometry of $5^+I_5^-{\cdot}2CH_2Cl_2$ in the crystal form (40% thermal ellipsoids; CH_2Cl_2, I_5, and H omitted for clarity).

= 1.812. It is notable that the g values of **3** and **4** are different from those of 2^+ ion, which is a N,O-chelate osmium(III) complex. However, the g values correlate well with those reported in the case of osmium(III) organometallic complexes.[26] The atomic spin obtained from Mulliken spin population analyses of 3^{Me} is solely localized on the osmium ion, as depicted in Figure 5c.

No iodination of the aromatic ring was observed in the **2** → **3** conversion. Moreover, the transformation of electrochemically generated 2^+ ion to **3** in solution discarded the notion of formation of a C–X bond as an intermediate for these ortho-metalation reactions in the presence of halogens. It is envisaged that the $Os(PPh_3)_2(CO)Br$ and $Os(PPh_3)_2Br_2$ units stabilize different electronic states, inducing different reactivities in **1** and **2**. One of the major differences in these two units is that the former contains a π-acidic CO ligand which stabilizes the monoanionic $PIQ^{\bullet-}$ state in **1** and even in the oxidized 1^+ ion, which is a $PIQ^{\bullet-}$ complex of osmium(III). However, the $PIQ^{\bullet-}$ state of **2** undergoes oxidation at relatively lower potential, forming a neutral PIQ chelate with osmium(III) ion. It is proposed that the $[Os^{III}(PPh_3)_2Br_2]$ unit prefers a monoanionic C,N compartment to a neutral N,O compartment, and the reaction as depicted in Chart 1 proceeds to the forward direction, slowly eliminating a proton. Halogenations of the aromatic ring are favorable with Br_2 and Cl_2 to I_2. In these reactions the ortho-metalated PIQ ligand undergoes bromination and chlorination in the presence of Br_2 and Cl_2, forming monobromo and dichloro derivatives. However, no aryl iodide was detected in this study.

$5^+I_5^-{\cdot}2CH_2Cl_2$ crystallizes in the space group $P2_1/n$. The molecular structure of the 5^+ ion in the crystal form and the atom-labeling scheme are illustrated in Figure 6. The average C–O lengths are 1.258(11) Å, while the C–C length of the chelate is 1.454(12) Å. The relatively shorter C–O and longer C–C lengths are similar to those of the PQ complexes of the types *trans*-$[Os^{II}(PQ)PPh_3(CO)Br]^+$ and *trans*-$[Ru^{II}(PQ)PPh_3(CO)Cl]^+$.[10] Thus, the 5^+ ion is defined as an osmium(III) complex of neutral PQ.

The higher stability of the PQ chelate over the PIQ with osmium(III) ion is predicted. The EPR spectrum of the frozen CH_2Cl_2 glass of $5^+I_5^-$ is illustrated in Figure S2c in the Supporting Information. The EPR g values are $g_1 = 2.500$, $g_2 = 2.030$, and $g_3 = 1.480$, which are consistent with the existence of osmium(III) ion in $5^+I_5^-$.

Electrochemical Studies. The redox activities of **1**–**4**, **6**, and 1^+ were investigated by cyclic voltammetry experiments in CH_2Cl_2 at 295 K, and redox potential data are summarized in Table 2. The cyclic voltammograms of **1**–**3** are illustrated in Figure 7, and the voltammograms of $1^+1/2I_3^-1/2Br^-$ and **4** are depicted in Figure S3 in the Supporting Information. The reversible anodic wave of **1** at +0.42 V is assigned to the Os^{III}/Os^{II} redox couple. Generally, the osmium(III)/osmium(II) redox potential notably depends on the coordinated-redox noninnocent ligand that promotes mixing of its low-lying π^* orbital with the d orbitals of osmium ion, shifting the charge to

DOI: 10.1021/acs.inorgchem.6b00040
Inorg. Chem. 2016, 55, 4746–4756

Table 2. Redox Potentials of 1, $1^+1/2I_3^-1/2Br^-$, 2, $3{\cdot}2CH_2Cl_2$ and $4{\cdot}2CH_2Cl_2$ Complexes Determined by Cyclic Voltammetry in CH_2Cl_2 Solution (0.20 M $[N(n\text{-}Bu)_4]PF_6$) at 295 K

	anodic wave ($E_{1/2}$, V)			cathodic wave ($E_{1/2}$, V)			
complex	$Os^{IV}(C,N\text{-}PIQ)/Os^{III}(C,N\text{-}PIQ)$ (ΔE,[a] mV)	$Os^{III}(PIQ^{\bullet-})/Os^{II}(PIQ^{\bullet-})$ (ΔE,[a] mV)	$Os^{III}(PIQ)/Os^{III}(PIQ^{\bullet-})$ (ΔE,[a] mV)	$Os^{II}(PIQ)/Os^{II}(PIQ^{\bullet-})$ (ΔE,[a] mV)	$Os^{III}(PIQ)/Os^{III}(PIQ^{\bullet-})$ (ΔE,[a] mV)	$Os^{III}(PIQ^{\bullet-})/Os^{III}(PIQ^{2-})$ (ΔE,[a] mV)	$Os^{II}(PIQ^{\bullet-})/Os^{II}(PIQ^{2-})$ (ΔE,[a] mV)
1		0.42 (90)		−0.52 (80)			−1.54[b]
$1^+1/2I_3^-1/2Br^-$			0.21 (150)			−1.22 (100)	
2			0.15 (80)			−1.21 (130)	
$3{\cdot}2CH_2Cl_2$	0.48 (110)				−0.80[b]		
$4{\cdot}2CH_2Cl_2$	0.46 (105)				−0.78[b]		

[a]Peak to peak separation. [b]Cathodic peak potential.

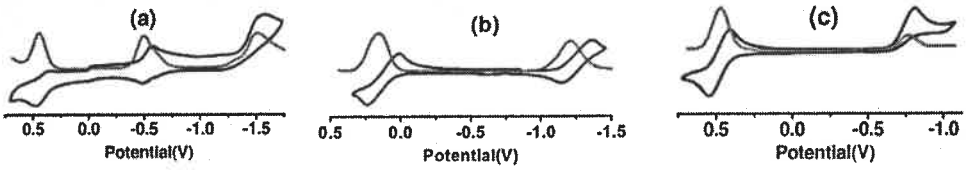

Figure 7. Cyclic voltammograms of (a) 1, (b) 2, and (c) 3 in CH_2Cl_2 at 295 K. Conditions: scan rate, 100 mV/s; 0.20 M $[N(n\text{-}Bu)_4]PF_6$ supporting electrolyte; platinum working electrode.

the ligand backbone. It was reported that the $[Os^{III}(L^{DAB})(PPh_3)_2Br_2]/[Os^{II}(L^{DAB})(PPh_3)_2Br_2]$ redox couple appeared at +0.34 V, with respect to the Fc^+/Fc redox couple, while the $[Os^{III}(L^{NHPh})(PPh_3)_2Br_2]/[Os^{II}(L^{NHPh})(PPh_3)_2Br_2]$ redox couple was found at −0.04 V (L^{DAB} = glyoxalbis(3-nitrophenyl)-imine and L^{NHPh} = glyoxalbis(*N*-phenyl)osazone).[27a−c] It was noteworthy that the Os^{II}/Os^{III} oxidation of *trans*-$[Os^{II}(DBQ)(PPh_3)_2(CO)Br]$ occurs at +0.46 V while Os^{III}/Os^{IV} oxidation of *trans*-$[Os^{III}(DBQ)(PPh_3)_2Br_2]$ occurs at +0.39 V, and the lower redox potential of the latter couple was analyzed by the effect of mixing of aromatic π^* orbital with the d orbitals of the osmium ion. To express the effect of the ligand vis á vis the metal ion, the redox couples of these complexes are defined by the [M(L)] combined state in this article. Thus, the anodic wave of **1** at +0.42 V is defined by the $Os^{III}(PIQ^{\bullet-})/Os^{II}(PIQ^{\bullet-})$ redox couple, instead of the Os^{III}/Os^{II} couple. Similarly, all other redox waves are assigned to a combined state, as summarized in Table 2. The single-crystal X-ray diffraction study of $1^+1/2I_3^-1/2Br^-$ revealed the $[Os^{III}(PIQ^{\bullet-})]$ state of the 1^+ ion. A significant feature of the voltammogram of **1** is that after a few scans (+1.0 to −1.3 V), a new cathodic wave appeared at −0.52 V which was initially absent but later emerged as a reversible and characteristic redox wave of **1**, as shown in Figure S3a. It is proposed that the anodic oxidation of $Os^{II}(PIQ^{\bullet-})$ to $Os^{III}(PIQ^{\bullet-})$ at +0.42 V generates a state of type $Os^{II}(PIQ)$ which is reversibly reduced at the cathode at −0.52 V. Thus, the generated cathodic wave at −0.52 V is assigned to the $Os^{II}(PIQ)/Os^{II}(PIQ^{\bullet-})$ redox couple. It was reported that the $PQ^{\bullet-}$ and azopyridine anion ($azp^{\bullet-}$) radical complexes of the types *cis*-/*trans*-$[M^{II}(PQ^{\bullet-})(PPh_3)_2(CO)X]$[10] and *trans*-$[M^{II}(azp^{\bullet-})(PPh_3)_2(CO)X]$[27d,e] exhibit similar types of cyclic voltammograms. The $[M^{II}(PQ)]/M^{II}(PQ^{\bullet-})]$ redox couples of the former complexes appear at +0.03 to −0.06 V vs Fc^+/Fc, while the $[M^{II}(azp)]/M^{II}(azp^{\bullet-})]$ redox couples were observed at −0.30 to −0.40 V vs SCE (M = Ru, Os; X = Cl, Br). The irreversible cathodic peak of **1** at −1.54 V is defined by the $Os^{II}(PIQ^{\bullet-})/Os^{II}(PIQ^{2-})$ redox couple. **2** exhibits one reversible anodic wave at +0.14 V, which is assigned to the $Os^{III}(PIQ)/Os^{III}(PIQ^{\bullet-})$ redox couple. The EPR spectra authenticated that 2^+ ion is a PIQ complex of osmium(III), while the 2^- ion is a PIQ^{2-} complex of osmium(III). Thus, the reversible cathodic wave of **2** at −1.21 V is designated by the $Os^{III}(PIQ^{\bullet-})/Os^{III}(PIQ^{2-})$ redox couple. The cyclic voltammogram of 1^+ ion is similar to that of **2**. The reversible $Os^{III}(PIQ)/Os^{III}(PIQ^{\bullet-})$ redox couple of 1^+ ion appears at +0.21 V, while the $Os^{III}(PIQ^{\bullet-})/Os^{III}(PIQ^{2-})$ couple attributes at −1.22 V. It is notable that the anodic and cathodic redox waves due to oxidation of I_3^- to I_2 and reduction of I_3^- to I^- are observed in the same range for $1^+1/2I_3^-1/2Br^-$ and the corresponding ruthenium complex,[27f] where the $M^{III}(PIQ^{\bullet-})/M^{II}(PIQ^{\bullet-})$ redox couples are not distinctly observable. The redox activities of **3**, **4**, and **6** are different, displaying only reversible anodic waves at +0.48, +0.46, and 0.52 V due to $Os^{IV}(C,N\text{-}PIQ)/Os^{III}(C,N\text{-}PIQ)$ redox couples, which are not observable in the cases of **1** and **2**. It is the effect of Os^{III}−Ar bond formation in **3** and **4** promoting mixing of the $\pi_{aromatic}{}^*$ orbitals with the osmium d orbitals[27a] that shifts the charge to the ligand backbone, facilitating oxidation at the anode. A MO of the mixing of a d orbital of the osmium ion with a π^* orbital of the ortho-metalated ligand is depicted in Figure S4 in the Supporting Information.

Electronic Spectra. UV/vis/NIR absorption spectra of the complexes in CH_2Cl_2 are shown in Figure S5 in the Supporting Information. The absorption parameters are summarized in Table 3. **1** exhibits absorption maxima at 580 and 412 nm. The corresponding calculated wavelengths (λ_{cal}) obtained from the TD DFT calculation (Table S4 in the Supporting Information) on $\mathbf{1}^{Me}$ in CH_2Cl_2 using the CPCM model are 650.9 nm due to $d_{Os} + p_{Br} \rightarrow \pi_{ISQ}$ (SOMO) and 489.8 nm due to π(SOMO) → $\pi^*_{Aromatic}$ transitions, which are defined as MLCT and ILCT transition types. The corresponding MLCT and ILCT transitions in **2** are red-shifted to 715 and 525 nm, and the λ_{cal} values for 2^{Me} are 931.32 (weaker) and 510.81 nm as metal to mixed-metal−ligand charge transfer (MMMLCT). Similar to the case for **2**, the 1^+ ion exhibits absorption maxima at 505 and 630 nm with a shoulder at 740 nm. The absorption spectra of **3**, **4**, and **6** are different from those of **1**, 1^+, and **2** and display

DOI: 10.1021/acs.inorgchem.6b00040
Inorg. Chem. 2016, 55, 4746−4756

Table 3. UV/Vis/NIR Absorption Spectral Data of 1, $1^+1/2I_3^-1/2Br^-$, 2, $3{\cdot}2CH_2Cl_2$, $4{\cdot}2CH_2Cl_2$, and 6 in CH_2Cl_2 at 295 K

complex	λ_{max} (nm) (ε (10^4 M^{-1} cm^{-1}))
1	770 (0.16), 580 (1.04), 412 (1.0), 302 (1.6), 260 (5.6)
$1^+1/2I_3^-1/2Br^-$	740 (0.55), 630 (0.7), 505 (0.97), 362 (2.40), 290 (4.0), 260 (5.7)
2	715 (0.47), 525 (1.6), 475 (1.2), 440 (1.04), 400 (1.04), 324 (1.92)
$3{\cdot}2CH_2Cl_2$	515 (0.67), 475 (0.56), 335 (0.66), 290 (1.10), 260 (3.35)
$4{\cdot}2CH_2Cl_2$	518 (0.76), 482 (0.65), 340 (0.57), 290 (0.96), 260 (3.66)
6	520 (0.82), 480 (0.66), 345 (0.70), 295 (1.28), 260 (4.06)
2^+	715 (0.52), 520 (1.22), 485 (1.32), 400 (1.26), 345 (1.68)
2^-	715 (0.60), 600 (0.83), 505 (1.02), 445 (1.04), 400 (1.17)

absorption maxima at 515 and 518 nm; the corresponding λ_{cal} value of 3^{Me} is 511.5 nm due to a $d_{Os} \rightarrow \pi_{IQ}$ transition. The changes in the electronic spectra during the conversions of $1 \rightarrow 1^+$, $2 \rightarrow 2^+$, and $2 \rightarrow 2^-$ were recorded by spectroelectrochemical measurements and are illustrated in Figure 8. $1 \rightarrow 1^+$ conversion undergoes several isosbestic points in the electronic spectra, as depicted in Figure 8a.

CONCLUSION

The article reports on the coordination chemistry of 9,10-phenanthreneiminoquinone (PIQ) with osmium containing triphenylphosphine, carbonyl, and halide as coligands. The study confirmed that the redox chemistry of PIQ is notably different from that of *o*-aminophenol derivatives and 9,10-phenanthrenequinone (PQ). A $PIQ^{\bullet-}$ complex of osmium(II) of type *trans*-$[Os^{II}(PIQ^{\bullet-})(PPh_3)_2(CO)Br]$ (1) was isolated, oxidation of which affords a osmium(III) complex of $PIQ^{\bullet-}$ of the type *trans*-$[Os^{III}(PIQ^{\bullet-})(PPh_3)_2(CO)Br]^+$ (1^+), while the corresponding PQ analogue is an osmium(II) complex of PQ of the type *trans*-$[Os^{II}(PQ)(PPh_3)_2(CO)Br]^+$. A $PIQ^{\bullet-}$ complex of osmium(III) of the type *trans*-$[Os^{III}(PIQ^{\bullet-})(PPh_3)_2Br_2]$ (2) was isolated, while the corresponding aminophenol analogue is a osmium(IV) complex of *o*-amidophenolato (AP^{2-}) of the type *trans*-$[Os^{IV}(AP^{2-})(PPh_3)_2Br_2]$. It was observed that in complexes the $PIQ^{\bullet-}$ state, in which a significant percentage of atomic spin is localized on the nitrogen p orbital (calculated, ~39% in 1), is more abundant than the PIQ and PIQ^{2-} states. PIQ is an ambidentate ligand, and the reactivities of 2 are also different from that of the PQ analogue *trans*-$[Os^{III}(PIQ^{\bullet-})(PPh_3)_2Br_2]$ (2_{PQ}). It was established that the conversion $[Os^{III}(PIQ^{\bullet-})] \rightarrow [Os^{III}(PIQ)]$ promotes Os^{III}–Ar bond formation. The phenomenon is defined as an iminosemiquinone to iminoquinone conversion promoted ortho-metalation reaction. In semiquinonate anion radical chemistry, this is a new observation. The oxidation of 2 with I_2, Br_2, and Cl_2 produces C,N-chelated complexes of the types *trans*-$[Os^{III}(C,N\text{-}PIQ)(PPh_3)_2Br_2]$ (3), *trans*-$[Os^{III}(C,N\text{-}PIQ^{Br})(PPh_3)_2Br_2]$ (4), and *trans*-$[Os^{III}(C,N\text{-}PIQ^{Cl2})(PPh_3)_2Br_2]$ (6) (C,N-PIQ = ortho-metalated PIQ, C,N-PIQ^{Br} = ortho-metalated 4-bromo PIQ, and C,N-PIQ^{Cl2} = ortho-metalated 3,4-dichloro PIQ). Similarly, the electrogenerated 2^+ ion in solution slowly furnishes 3. In contrast, the reaction of 2_{PQ} with I_2 affords a PQ complex of the type *trans*-$[Os^{III}(PQ)(PPh_3)_2Br_2]^+$ (5^+). In this case no ortho-metalation reaction is established. Thus, this work discloses that PIQ is a redox-noninnocent ligand which incites redox state dependent ortho-metalation reactions with osmium(III) ion.

ASSOCIATED CONTENT

Supporting Information

The Supporting Information is available free of charge on the ACS Publications website at DOI: 10.1021/acs.inorgchem.6b00040.

EPR data, cyclic voltammograms, UV/vis/NIR spectra, gas-phase optimized coordinates of 1^{Me}, 1^{Me+}, 2^{Me}, 2^{Me+}, 2^{Me-}, and 3^{Me}, excitation energies, and oscillator strengths, transition types, and dominant contributions of UV/vis/NIR absorption bands from TD DFT calculations (PDF)

X-ray crystallographic data for the complexes 1, $1^+1/2I_3^-1/2Br^-$, 2, $3{\cdot}2CH_2Cl_2$ $4{\cdot}CH_2Cl_2$ $5^+I_5^-{\cdot}2CH_2Cl_2$ and 6 (ZIP)

AUTHOR INFORMATION

Corresponding Author

*P.G.: e-mail, ghosh@pghosh.in; tel, +91-33-2428-7347; fax, +91-33-2477-3597.

Author Contributions

The manuscript was written through contributions of all authors. All authors have given approval to the final version of the manuscript.

Notes

The authors declare no competing financial interest.

ACKNOWLEDGMENTS

Financial support was received from the Department of Science and Technology (SR/S1/IC/0026/2012) and Council of Scientific and Industrial Research 01(2699/12/EMR-II), New Delhi, India. S.B. (08/531(0006)/2012-EMR-I), S.M. (No. F. 11-24/2013/SA-I and F.D. Dy. No.766/FRD-III), and S.M.

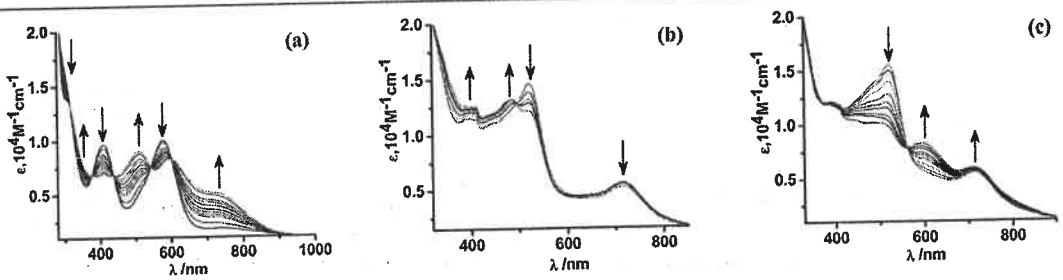

Figure 8. Spectroelectrochemical measurements showing the change in electronic spectra during the conversions of (a) $1 \rightarrow 1^+$, (b) $2 \rightarrow 2^+$, and (c) $2 \rightarrow 2^-$ CH_2Cl_2 at 295 K.

DOI: 10.1021/acs.inorgchem.6b00040
Inorg. Chem. 2016, 55, 4746–4756

(08/531(0004)/2010-EMR-I) are grateful to the CSIR/UGC, New Delhi, India, for fellowships.

REFERENCES

(1) (a) Tang, Z.; Otten, E.; Reek, J. N. H.; van der Vlugt, J. I.; de Bruin, B. *Chem. - Eur. J.* **2015**, *21*, 12683–12693. (b) Broere, D. L. J.; Metz, L. L.; de Bruin, B.; Reek, J. N. H.; Siegler, M. A.; van der Vlugt, J. I. *Angew. Chem., Int. Ed.* **2015**, *54*, 1516–1520. (c) Jacquet, J.; Salanouve, E.; Orio, M.; Vezin, H.; Blanchard, S.; Derat, E.; Desage-El Murr, M.; Fensterbank, L. *Chem. Commun.* **2014**, *50*, 10394–10397. (d) Mukherjee, C.; Weyhermüller, T.; Bothe, E.; Chaudhuri, P. *Inorg. Chem.* **2008**, *47*, 2740–2746.

(2) (a) Broere, D. L. J.; Plessius, R.; van der Vlugt, J. I. *Chem. Soc. Rev.* **2015**, *44*, 6886–6915. (b) Leenders, S. H. A. M.; Gramage-Doria, R.; de Bruin, B.; Reek, J. N. H. *Chem. Soc. Rev.* **2015**, *44*, 433–448. (c) Poneti, G.; Poggini, L.; Mannini, M.; Cortigiani, B.; Sorace, L.; Otero, E.; Sainctavit, P.; Magnani, A.; Sessoli, R.; Dei, A. *Chem. Sci.* **2015**, *6*, 2268–2274. (d) Parthey, M.; Kaupp, M. *Chem. Soc. Rev.* **2014**, *43*, 5067–5088. (e) Tezgerevska, T.; Alley, K. G.; Boskovic, C. *Coord. Chem. Rev.* **2014**, *268*, 23–40. (f) Luca, O. R.; Crabtree, R. H. *Chem. Soc. Rev.* **2013**, *42*, 1440–1459. (g) Suarez, A. I. O.; Lyaskovskyy, V.; Reek, J. N. H.; van der Vlugt, J. I.; de Bruin, B. *Angew. Chem., Int. Ed.* **2013**, *52*, 12510–12529. (h) Kaim, W.; Schwederski, B. *Coord. Chem. Rev.* **2010**, *254*, 1580–1588. (i) Bill, E.; Bothe, E.; Chaudhuri, P.; Chlopek, K.; Herebian, D.; Kokatam, S.; Ray, K.; Weyhermüller, T.; Neese, F.; Wieghardt, K. *Chem. - Eur. J.* **2005**, *11*, 204–224. (k) Herebian, D.; Wieghardt, K.; Neese, F. *J. Am. Chem. Soc.* **2003**, *125*, 10997–11005. (j) Hendrickson, D. N.; Pierpont, C. G.; Gütlich, P.; Goodwin, H. A. *Top. Curr. Chem.* **2004**, *234*, 63–95.

(3) (a) Kundu, S.; Maity, S.; Weyhermüller, T.; Ghosh, P. *Inorg. Chem.* **2013**, *52*, 7417–7430. (b) Pierpont, C. G. *Inorg. Chem.* **2011**, *50*, 9766–9772. (c) Suenaga, Y.; Pierpont, C. G. *Inorg. Chem.* **2005**, *44*, 6183–6191. (d) Pierpont, C. G. *Coord. Chem. Rev.* **2001**, *216–217*, 99. (e) Pierpont, C. G. *Coord. Chem. Rev.* **2001**, *219–221*, 415–433.

(4) (a) Kochem, A.; Gellon, G.; Jarjayes, O.; Philouze, C.; d'Hardemare, A. M.; Gastel, M.; Thomas, F. *Dalton Trans.* **2015**, *44*, 12743–12756. (b) Piskunov, A. V.; Meshcheryakova, I. N.; Ershova, I. V.; Bogomyakov, A. S.; Cherkasov, A. V.; Fukin, G. K. *RSC Adv.* **2014**, *4*, 42494–42505. (c) Rajput, A.; Sharma, A. K.; Barman, S. K.; Koley, D.; Steinert, M.; Mukherjee, R. *Inorg. Chem.* **2014**, *53*, 36–48. (d) Rakshit, R.; Ghorai, S.; Biswas, S.; Mukherjee, C. *Inorg. Chem.* **2014**, *53*, 3333–3337. (e) Bubrin, M.; Schweinfurth, D.; Ehret, F.; Záliš, S.; Kvapilová, H.; Fiedler, J.; Zeng, Q.; Hartl, F.; Kaim, W. *Organometallics* **2014**, *33*, 4973–4985. (f) Kundu, S.; Maity, S.; Maity, A. N.; Ke, S.-C.; Ghosh, P. *Dalton Trans.* **2013**, *42*, 4586–4601. (g) Bittner, M. M.; Kraus, D.; Lindeman, S. V.; Popescu, C. V.; Fiedler, A. T. *Chem. - Eur. J.* **2013**, *19*, 9686–9698. (h) Saha Roy, A.; Saha, P.; Adhikary, N. D.; Ghosh, P. *Inorg. Chem.* **2011**, *50*, 2488–2500. (i) Poddel'sky, A. I.; Cherkasov, V. K.; Abakumov, G. A. *Coord. Chem. Rev.* **2009**, *253*, 291–324. (j) Remenyi, C.; Kaupp, M. *J. Am. Chem. Soc.* **2005**, *127*, 11399–11413. (k) Min, K. S.; Weyhermüller, T.; Bothe, E.; Wieghardt, K. *Inorg. Chem.* **2004**, *43*, 2922–2931. (l) Sun, X.; Chun, H.; Hildenbrand, K.; Bothe, E.; Weyhermüller, T.; Neese, F.; Wieghardt, K. *Inorg. Chem.* **2002**, *41*, 4295–4303.

(5) (a) Ciccione, J.; Leconte, N.; Luneau, D.; Philouze, C.; Thomas, F. *Inorg. Chem.* **2016**, *55*, 649–665. (b) Skara, G.; Pinter, B.; Geerlings, P.; De Proft, F. *Chem. Sci.* **2015**, *6*, 4109–4117. (c) Leconte, N.; Ciccione, J.; Gellon, G.; Philouze, C.; Thomas, F. *Chem. Commun.* **2014**, *50*, 1918–1920. (d) Robinson, S.; Davies, E. S.; Lewis, W.; Blake, A. J.; Liddle, S. T. *Dalton Trans.* **2014**, *43*, 4351–4360. (e) Kapovsky, M.; Dares, C.; Dodsworth, E. S.; Begum, R. A.; Raco, V.; Lever, A. B. P. *Inorg. Chem.* **2013**, *52*, 169–181. (f) Kochem, A.; Gellon, G.; Leconte, N.; Baptiste, B.; Philouze, C.; Jarjayes, O.; Orio, M.; Thomas, F. *Chem. - Eur. J.* **2013**, *19*, 16707–16721. (g) Lever, A. B. P. *Coord. Chem. Rev.* **2010**, *254*, 1397–1405. (h) Shimazaki, Y.; Stack, T. D. P.; Storr, T. *Inorg. Chem.* **2009**, *48*, 8383–8392. (i) Herebian, D.; Bothe, E.; Neese, F.; Weyhermüller, T.; Wieghardt, K. *J. Am. Chem. Soc.* **2003**, *125*, 9116–9128.

(6) (a) Metzinger, R.; Demeshko, S.; Limberg, C. *Chem. - Eur. J.* **2014**, *20*, 4721–4735. (b) Cipressi, J.; Brown, S. N. *Chem. Commun.* **2014**, *50*, 7956–7959. (c) Hänninen, M. M.; Paturi, P.; Tuononen, H. M.; Sillanpää, R.; Lehtonen, A. *Inorg. Chem.* **2013**, *52*, 5714–5721. (d) Piskunov, A. V.; Trofimova, O. Y.; Fukin, G. K.; Ketkov, S. Y.; Smolyaninov, I. V.; Cherkasov, V. K. *Dalton Trans.* **2012**, *41*, 10970–10979. (e) Szigethy, G.; Shaffer, D. W.; Heyduk, A. F. *Inorg. Chem.* **2012**, *51*, 12606–12618. (f) Brown, S. N. *Inorg. Chem.* **2012**, *51*, 1251–1260. (g) Mukherjee, C.; Weyhermüller, T.; Bothe, E.; Chaudhuri, P. *Inorg. Chem.* **2008**, *47*, 11620–11632. (h) Chaudhuri, P.; Bill, E.; Wagner, R.; Pieper, U.; Biswas, B.; Weyhermüller, T. *Inorg. Chem.* **2008**, *47*, 5549–5551.

(7) (a) Mandal, A.; Kundu, T.; Ehret, F.; Bubrin, M.; Mobin, S. M.; Kaim, W.; Lahiri, G. K. *Dalton Trans.* **2014**, *43*, 2473–2487.

(8) (a) César, V.; Mallardo, V.; Nano, A.; Dahm, G.; Lugan, N.; Lavigne, G.; Bellemin-Laponnaz, S. *Chem. Commun.* **2015**, *51*, 5271–5274. (b) Ghosh, P.; Ray, R.; Das, A.; Lahiri, G. K. *Inorg. Chem.* **2014**, *53*, 10695–10707. (c) Kobayashi, A.; Fukuzawa, Y.; Chang, H.-C.; Kato, M. *Inorg. Chem.* **2012**, *51*, 7508–7519. (d) Rachford, A. A.; Petersen, J. L.; Rack, J. J. *Inorg. Chem.* **2006**, *45*, 5953–5960. (e) Buckingham, D. A.; Creaser, I. I.; Sargeson, A. M. *Inorg. Chem.* **1970**, *9*, 655–661. (f) Werner, A. *Ber. Dtsch. Chem. Ges.* **1907**, *40*, 765–788.

(9) (a) Díaz-Álvarez, A. E.; Vidal, C.; Suárez, F. J.; Díez, J.; Cadierno, V.; Crochet, P. *Organometallics* **2015**, *34*, 3670–3677. (b) Sinha, A.; Majumdar, M.; Sarkar, M.; Ghatak, T.; Bera, J. K. *Organometallics* **2013**, *32*, 340–349. (c) Chung, L.-H.; Wong, C.-Y. *Organometallics* **2013**, *32*, 3583–3586. (d) Sarkar, M.; Doucet, H.; Bera, J. K. *Chem. Commun.* **2013**, *49*, 9764–9766. (e) Sugimoto, H.; Ashikari, K.; Itoh, S. *Inorg. Chem.* **2013**, *52*, 543–545. (f) Labande, A.; Debono, N.; Sournia-Saquet, A.; Daran, J.-C.; Poli, R. *Dalton Trans.* **2013**, *42*, 6531–6537. (g) Chung, L.-H.; Chan, S.-C.; Lee, W.-C.; Wong, C.-Y. *Inorg. Chem.* **2012**, *51*, 8693–8703. (h) Rahaman, S. M. W.; Dinda, S.; Ghatak, T.; Bera, J. K. *Organometallics* **2012**, *31*, 5533–5540. (i) Donnelly, K. F.; Lalrempuia, R.; Müller-Bunz, H.; Albrecht, M. *Organometallics* **2012**, *31*, 8414–8419.

(10) (a) Biswas, M. K.; Patra, S. C.; Maity, A. N.; Ke, S.-C.; Weyhermüller, T.; Ghosh, P. *Dalton Trans.* **2013**, *42*, 6538–6552. (b) Biswas, M. K.; Patra, S. C.; Maity, A. N.; Ke, S.-C.; Adhikary, N. D.; Ghosh, P. *Inorg. Chem.* **2012**, *51*, 6687–6699.

(11) (a) Ahmad, N.; Levison, J. J.; Robinson, S. D.; Uttley, M. F. *Inorg. Synth.* **2007**, *15*, 45. (b) Hoffman, P. R.; Caulton, K. G. *J. Am. Chem. Soc.* **1975**, *97*, 4221.

(12) (a) Schmidt, J.; Junghans, E. *Ber. Dtsch. Chem. Ges.* **1904**, *37*, 3558. (b) Pschorr, R. *Ber. Dtsch. Chem. Ges.* **1902**, *35*, 2729.

(13) (a) Sheldrick, G. M. *ShelXS97*; Universität Göttingen, Göttingen, Germany, 1997. (b) Sheldrick, G. M. *ShelXL97*; Universität Göttingen, Göttingen, Germany, 1997. (c) Sheldrick, G. M. *XS. Version 2013/1*; Georg-August-Universität Göttingen, Göttingen, Germany, 2013. (d) Sheldrick, G. M. *Acta Crystallogr., Sect. A: Found. Adv.* **2015**, *71*, 3–8. (e) Sheldrick, G. M. *Acta Crystallogr., Sect. C: Struct. Chem.* **2015**, *71*, 3–8.

(14) Frisch, M. J.; Trucks, G. W.; Schlegel, H. B.; Scuseria, G. E.; Robb, M. A.; Cheeseman, J. R.; Montgomery, J. A., Jr.; Vreven, T.; Kudin, K. N.; Burant, J. C.; Millam, J. M.; Iyengar, S. S.; Tomasi, J.; Barone, V.; Mennucci, B.; Cossi, M.; Scalmani, G.; Rega, N.; Petersson, G. A.; Nakatsuji, H.; Hada, M.; Ehara, M.; Toyota, K.; Fukuda, R.; Hasegawa, J.; Ishida, M.; Nakajima, T.; Honda, Y.; Kitao, O.; Nakai, H.; Klene, M.; Li, X.; Knox, J. E.; Hratchian, H. P.; Cross, J. B.; Bakken, V.; Adamo, C.; Jaramillo, J.; Gomperts, R.; Stratmann, R. E.; Yazyev, O.; Austin, A. J.; Cammi, R.; Pomelli, C.; Ochterski, J. W.; Ayala, P. Y.; Morokuma, K.; Voth, G. A.; Salvador, P.; Dannenberg, J. J.; Zakrzewski, V. G.; Dapprich, S.; Daniels, A. D.; Strain, M. C.; Farkas, O.; Malick, D. K.; Rabuck, A. D.; Raghavachari, K.; Foresman, J. B.; Ortiz, J. V.; Cui, Q.; Baboul, A. G.; Clifford, S.; Cioslowski, J.; Stefanov, B. B.; Liu, G.; Liashenko, A.; Piskorz, P.; Komaromi, I.; Martin, R. L.; Fox, D. J.; Keith, T.; Al-Laham, M. A.; Peng, C. Y.; Nanayakkara, A.; Challacombe, M.; Gill, P. M. W.; Johnson, B.; Chen,

DOI: 10.1021/acs.inorgchem.6b00040
Inorg. Chem. 2016, 55, 4746–4756

W.; Wong, M. W.; Gonzalez, C.; Pople, J. A. *Gaussian 03, Revision E.01*; Gaussian, Inc., Wallingford, CT, 2004.
(15) (a) Parr, R. G.; Yang, W. *Density Functional Theory of Atoms and Molecules*; Oxford University Press: Oxford, U.K., 1989. (b) Salahub, D. R.; Zerner, M. C. *The Challenge of d and f Electrons*; American Chemical Society: Washington, DC, 1989; ACS Symposium Series 394. (c) Kohn, W.; Sham, L. *Phys. Rev.* **1965**, *140*, A1133. (d) Hohenberg, P.; Kohn, W. *Phys. Rev.* **1964**, *136*, B864.
(16) (a) Stratmann, R. E.; Scuseria, G. E.; Frisch, M. *J. Chem. Phys.* **1998**, *109*, 8218. (b) Casida, M. E.; Jamorski, C.; Casida, K. C.; Salahub, D. R. *J. Chem. Phys.* **1998**, *108*, 4439. (c) Bauernschmitt, R.; Haser, M.; Treutler, O.; Ahlrichs, R. *Chem. Phys. Lett.* **1996**, *256*, 454.
(17) (a) Becke, A. D. *J. Chem. Phys.* **1993**, *98*, 5648. (b) Miehlich, B.; Savin, A.; Stoll, H.; Preuss, H. *Chem. Phys. Lett.* **1989**, *157*, 200. (c) Lee, C.; Yang, W.; Parr, R. G. *Phys. Rev. B: Condens. Matter Mater. Phys.* **1988**, *37*, 785.
(18) Pulay, P. *J. Comput. Chem.* **1982**, *3*, 556.
(19) Schlegel, H. B.; McDouall, J. J. In *Computational Advances in Organic Chemistry*; Ogretir, C., Csizmadia, I. G., Eds.; Kluwer Academic: Dordrecht, The Netherlands, 1991; pp 167−185.
(20) (a) Hay, P. J.; Wadt, W. R. *J. Chem. Phys.* **1985**, *82*, 270. (b) Wadt, W. R.; Hay, P. J. *J. Chem. Phys.* **1985**, *82*, 284. (c) Hay, P. J.; Wadt, W. R. *J. Chem. Phys.* **1985**, *82*, 299.
(21) (a) Rassolov, V. A.; Ratner, M. A.; Pople, J. A.; Redfern, P. C.; Curtiss, L. A. *J. Comput. Chem.* **2001**, *22*, 976. (b) Francl, M. M.; Pietro, W. J.; Hehre, W. J.; Binkley, J. S.; DeFrees, D. J.; Pople, J. A.; Gordon, M. S. *J. Chem. Phys.* **1982**, *77*, 3654. (c) Hariharan, P. C.; Pople, J. A. *Mol. Phys.* **1974**, *27*, 209. (d) Hariharan, P. C.; Pople, J. A. *Theor. Chim. Acta.* **1973**, *28*, 213.
(22) Hehre, W. J.; Ditchfield, R.; Pople, J. A. *J. Chem. Phys.* **1972**, *56*, 2257.
(23) See the single-crystal X-ray bond parameters of [Ru^{III}(PIQ)PPh_3Br_3] (CCDC No. 1442786).
(24) Bhattacharya, S.; Gupta, P.; Basuli, F. *Inorg. Chem.* **2002**, *41*, 5810−5816.
(25) (a) Ghosh, P.; Pramanik, K.; Chakravorty, A. *J. Chem. Soc., Chem. Commun.* **1995**, 4, 477−478. (b) Mandal, A.; Grupp, A.; Schwederski, B.; Kaim, W.; Lahiri, G. K. *Inorg. Chem.* **2015**, *54*, 7936−7944. (c) Das, D.; Sarkar, B.; Mondal, T. K.; Mobin, S. M.; Fiedler, J.; Kaim, W.; Lahiri, G. K. *Inorg. Chem.* **2011**, *50*, 7090−7098. (d) Samanta, S.; Singh, P.; Fiedler, J.; Záliš, S.; Kaim, W.; Goswami, S. *Inorg. Chem.* **2008**, *47*, 1625−1633.
(26) (a) Albrecht, M. *Chem. Rev.* **2010**, *110*, 576−623. (b) Panda, B. K. *Open J. Inorg. Chem.* **2012**, *02*, 49−57.
(27) (a) Maity, S.; Kundu, S.; Weyhermüller, T.; Ghosh, P. *Inorg. Chem.* **2015**, *54*, 1384−1394. (b) Patra, S. C.; Weyhermüller, T.; Ghosh, P. *Inorg. Chem.* **2014**, *53*, 2427−2440. (c) Patra, S. C.; Saha Roy, A.; Manivannan, V.; Weyhermüller, T.; Ghosh, P. *Dalton Trans.* **2014**, *43*, 13731−13741. (d) Shivakumar, M.; Pramanik, K.; Ghosh, P.; Chakravorty, A. *Inorg. Chem.* **1998**, *37*, 5968−5969. (e) Pramanik, K.; Shivakumar, M.; Ghosh, P.; Chakravorty, A. *Inorg. Chem.* **2000**, *39*, 195−199. (f) Bera, S.; Maity, S.; Weyhermüller, T.; Ghosh, P. *Dalton Trans.* **2016**, DOI: 10.1039/C6DT00091F.

DOI: 10.1021/acs.inorgchem.6b00040
Inorg. Chem. 2016, 55, 4746−4756